JOURNAL OF AGRICULTURAL AND FOOD CHEMISTRY

Inhibition of Lactoperoxidase-Catalyzed 2,2′-Azino-bis(3-ethylbenzthiazoline-6-sulfonic acid) (ABTS) and Tyrosine Oxidation by Tyrosine-Containing Random Amino Acid Copolymers

MORTEN R. CLAUSEN,[‡] LEIF H. SKIBSTED,[§] AND JAN STAGSTED*,[‡]

Department of Food Science, Faculty of Agricultural Sciences, University of Aarhus, 8830 Tjele, Denmark, and Department of Food Science, Faculty of Life Sciences, University of Copenhagen, 1165 Copenhagen, Denmark

Oxidation of 2,2′-azino-bis(3-ethylbenzthiazoline-6-sulfonic acid) by lactoperoxidase was found to be inhibited by tyrosine-containing random amino acid copolymers but not by tyrosine. Both electrostatic effects and polymer size were found to be important by comparison of negatively and positively charged copolymers of varying lengths, with poly(Glu, Tyr)4:1 ($[E_4Y_1]_{\sim 40}$) as the strongest competitive inhibitor (EC_{50} ~20 nM). This polymer did not form dityrosine in the presence of lactoperoxidase (LPO) and peroxide. Furthermore, incubation with *tert*-butyl hydroperoxide, as opposed to hydrogen peroxide, resulted in a peculiar long lag phase of the reaction between the redox intermediate compound II and $[E_4Y_1]_{\sim 40}$, indicating a very tight association between enzyme and inhibitor. We propose that interactions between multiple positively charged areas on the surface of LPO and the polymer are required for optimal inhibition.

KEYWORDS: Lactoperoxidase; ABTS; tyrosine; random amino acid copolymer; dityrosine

INTRODUCTION

Lactoperoxidase (LPO, EC 1.11.1.7) is found on mucosal surfaces and in secretory fluids, such as milk, saliva, and tears of mammals, where it exerts antibacterial activity through the formation of hypohalides and hypothiocyanite from the corresponding halides and thiocyanate, respectively (*1*). A number of organic compounds including several of biological relevance, such as tyrosine and other phenolic compounds, have been identified as electron donors for LPO-mediated reduction of peroxides (*2*). Oxidation of tyrosine results in the formation of dityrosine, and proteins may become cross-linked, resulting in structural and functional changes (*3*). LPO may also induce oxidation of glutathione and lipid peroxidation in membranes and cause hemolysis (*4*−*6*). Recently, it was shown that LPO catalyzes the decomposition of lipid hydroperoxides, resulting in the formation of singlet oxygen ($^1O_2$) and peroxyl radicals, thus promoting lipid oxidation (*7*).

LPO is activated by hydrogen peroxide through the initial formation of the strongly oxidizing intermediate compound I (Cpd I), reaction 1 (*8, 9*). In the case of tyrosine oxidation, two consecutive one-electron reactions subsequently convert two tyrosines to tyrosyl radicals and reduce Cpd I stepwise to Cpd II and native enzyme (*8, 10*), reactions 2 and 3.

$$\text{LPO} + H_2O_2 \rightarrow \text{Cpd I } [{}^{+}\text{Fe}^{\text{IV}}{=}\text{O}] + H_2O \quad (1)$$

$$\text{Cpd I } [{}^{\bullet+}\text{Fe}^{\text{IV}}{=}\text{O}] + \text{tyrosine} \rightarrow \text{Cpd II } [\text{Fe}^{\text{IV}}{=}\text{O}] + \text{tyrosyl radical} \quad (2)$$

$$\text{Cpd II } [\text{Fe}^{\text{IV}}{=}\text{O}] + \text{tyrosine} \rightarrow \text{LPO} + \text{tyrosyl radical} \quad (3)$$

Tyrosyl radicals leave the active site of the enzyme in a diffusion-controlled reaction and may react via a radical recombination mechanism to form *o*,*o*′-dityrosine (*10*).

2,2′-Azino-bis(3-ethylbenzthiazoline-6-sulfonic acid) (ABTS) is often used as a one-electron donor to assess LPO activity because of the formation of the *meta*-stable and colored free-radical ion $ABTS^{\bullet+}$. The steady-state kinetics of peroxidase-catalyzed oxidation of ABTS was first described by Bardsley's group (*11*−*13*) and later critically re-evaluated (*14*). The dependence on H_2O_2 and ABTS concentration is complex because of enzyme inactivation at high substrate concentrations, and in the case of LPO, aggregation further complicates the kinetic analysis (*13, 14*).

The synthetic polymer poly(Glu,Tyr) ($[EY]_n$) is an excellent substrate for tyrosine kinases (*15, 16*), and we considered this

* To whom correspondence should be addressed: Department of Food Science, University of Aarhus, Blichers Alle 20, DK-8830 Tjele, Denmark. Telephone: ++45-89991186. Fax: ++45-89991564. E-mail: jan.stagsted@agrsci.dk.

[‡] University of Aarhus.

[§] University of Copenhagen.

10.1021/jf801582e CCC: $40.75
Published on Web 08/30/2008

polymer as a model for studies of the formation of dityrosine cross-links in proteins. However, according to Malencik and Anderson (*17*), various peroxidases, including LPO, do not catalyze dityrosine formation in $[E_4Y_1]_{\sim 40}$. Surprisingly, we found that these polymers very effectively compete with ABTS as electron donors for LPO.

MATERIALS AND METHODS

Materials. ABTS, hydrogen peroxide, *tert*-butyl hydroperoxide, tyrosine, $[E_4Y_1]_{\sim 40}$ (corresponding to M_w = 20−50 kDa), $[E_4Y_1]_{\sim 20}$ (corresponding to M_w = 5−20 kDa), $[E_1Y_1]_{\sim 100}$, $[K_4Y_1]_{\sim 40}$, and $[E_3A_2]_{\sim 50}$ (all corresponding to M_w = 20−50 kDa) were from Sigma Aldrich (Steinheim, Germany) and used without further purification. LPO was purified from freshly collected bovine milk from the herd at Foulum, University of Aarhus, by cation-exchange chromatography (absorbance ratio at 412/280 nm ∼ 0.60). The LPO preparation was further purified by size-exclusion chromatography (SEC) on a Phenomenex BioSep 3000 column (300 mm × 7.0 mm × 5 μm) (Barcelona, Spain) on a high-pressure liquid chromatography system (HP 1100, Agilent Technologies, Palo Alto, CA) using 10 mM phosphate buffer at pH 7.4 with 0.15 M NaCl as the mobile phase. Peak fractions were collected and pooled, and an $A_{412/280}$ value of 0.85 was obtained. The pooled LPO was dialysed against the assay buffer (50 mM phosphate at pH 6.0).

ABTS Oxidation in the Presence of Polymers. LPO activity was measured on a PowerWave$_X$ microplate scanning spectrophotometer from Bio-Tek Instruments, Inc. (Winooski, VT) with the KC4 software for data analysis. ABTS (18.8 mM) was dissolved in deionized water (18.2 MΩ), and the concentration was determined spectrophotometrically using $\varepsilon_{340\ nm} = 3.6 \times 10^4\ M^{-1}\ cm^{-1}$ (*11*) and stored at −20 °C. Polymers were dissolved in 50 mM phosphate buffer at pH 6.0, and the tyrosine concentrations were determined using $\varepsilon_{275\ nm} = 1400\ M^{-1}\ cm^{-1}$ (*18*). Lactoperoxidase concentration was determined using $\varepsilon_{412\ nm} = 1.12 \times 10^5\ M^{-1}\ cm^{-1}$ (*19*) and diluted to a final concentration of 3.0 nM in 50 mM phosphate buffer at pH 6.0. LPO was mixed with stock solutions of ABTS and polymer, and the reactions were initiated by the addition of H_2O_2 to a final concentration of 50 μM from a stock, where the concentration of hydrogen peroxide was determined using $\varepsilon_{240\ nm} = 39.4\ M^{-1}\ cm^{-1}$ (*20*). All reactions were followed at 30 °C in 96-well microplates from Bibby Sterilin Ltd. (Stone, Staffordshire, U.K.). The rate of $ABTS^{\bullet+}$ formation was determined as $\Delta A_{414}/\Delta$min, and absorbance readings within the first minute were converted to initial reaction rates using the $\varepsilon_{414\ nm} = 3.6 \times 10^4\ M^{-1}\ cm^{-1}$ for $ABTS^{\bullet+}$ (*11*).

Polymer Size. A mixture of high-molecular-weight (HMW) and low-molecular-weight (LMW) preparations of $[E_4Y_1]_n$ were subjected to SEC as described above for LPO, and fractions (200 μL) were collected with a G1364C fraction collector from Agilent. LPO activity in the presence of the fractions at different concentrations was used to determine the half-maximal inhibition (EC_{50}) values as a function of elution volume from SEC. Molecular weights of selected fractions of the polymer were determined using matrix-assisted laser desorption−ionization time-of-flight (MALDI−TOF) as the mass with the highest intensity in the spectra using the following procedure: Samples (0.5 μL) were applied to a MTP AnchorChip (Bruker Daltonics, Bremen, Germany) and allowed to dry followed by the addition of 1.0 μL of 10% formic acid and 0.5 μL of matrix, either 20 mg/mL 3-(4-hydroxy-3,5-dimethoxyphenyl)prop-2-enoic acid in 50% acetonitrile or α-cyano-4-hydroxycinnamic acid in 70% acetonitrile, dependent upon polymer size. Ions were detected with a Bruker Ultraflex MALDI−TOF tandem mass spectrometer equipped with a 337 nm nitrogen laser in positive mode. The instrument was operated in reflector mode for the LMW samples and linear mode for the HMW samples, with an accelerating voltage of 25 kV. Results were analyzed by Flex Analysis software version 2.4 (Bruker Daltonics).

Kinetic Experiments. Tyrosine (1.5 mM) and $[E_4Y_1]_{\sim 40}$ (1.5 mM tyrosine equivalents) were dissolved in aqueous 50 mM phosphate at pH 6.0. LPO (3 nM) and stock solutions were mixed to yield the following concentrations, ABTS (60−280 μM) and tyrosine (0.41−300 μM) or $[E_4Y_1]_{\sim 40}$ (0.41−300 nM tyrosine equivalents) in 50 mM phosphate buffer at pH 6.0. The reaction was initiated by the addition of 50 μM H_2O_2, and the apparent LPO activity was determined as described above.

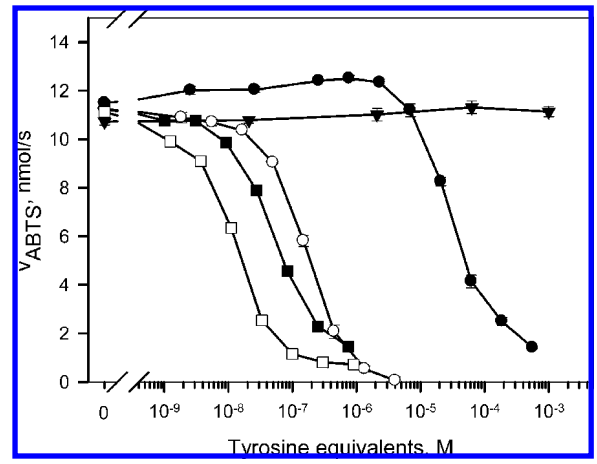

Figure 1. Effect of glutamate/tyrosine or lysine/tyrosine random copolymers or a mixture of free glutamate and tyrosine (molar ratio of 4:1) (▼) on LPO-mediated ABTS oxidation by H_2O_2 in aqueous solution at pH 6.0 and 30 °C. $[K_4Y_1]_{\sim 40}$ (●), $[E_1Y_1]_{\sim 100}$ (○), $[E_4Y_1]_{\sim 20}$ (■), and $[E_4Y_1]_{\sim 40}$ (□). Means ± standard error of the mean (SEM) from three experiments are shown.

Reaction of $[E_4Y_1]_{\sim 40}$ with Cpd II. Because of the long half-life of Cpd II (*21*), the reaction of $[E_4Y_1]_{\sim 40}$ with this enzyme intermediate of LPO was studied spectrophotometrically. LPO (1.0 μM) was mixed with 2.0 μM hydrogen peroxide or 3.0 mM *tert*-butyl hydroperoxide, and the formation of Cpd II was confirmed at 430 nm on a HP8453 diode array spectrophotometer. The decay of Cpd II without the addition of an electron donor was negligible within the observed period, and the reaction of this LPO redox intermediate was determined at room temperature in a quartz cuvette in the spectrophotometer following manual addition of tyrosine or $[E_4Y_1]_{\sim 40}$ (0.2 mM). Absorbance at 412 nm was used to detect the formation of native LPO, and a decrease in absorbance at 430 nm was used to detect a decay of Cpd II. In parallel experiments, the formation of dityrosine was determined with a Perkin-Elmer LS 50B luminescence spectrometer (Perkin-Elmer, Beaconsfield, U.K.) with 0.5 × 0.5 cm quartz cuvettes, with excitation at 315 nm and emission at 400 nm.

LPO (1.0 μM) was also pre-incubated with tyrosine or $[E_4Y_1]_{\sim 40}$ (0.2 mM) for 30 min at room temperature followed by the addition of hydrogen peroxide (3.0 μM) or *tert*-butyl hydroperoxide (3.0 mM), and the reaction intermediates of LPO were determined as described above.

Dityrosine Formation. Tyrosine, $[E_4Y_1]_{\sim 40}$ (both 0.5 mM), or mixtures of both in 50 mM phosphate buffer at pH 6.0 were mixed with LPO and H_2O_2 to yield concentrations of 0.38 and 50 μM, respectively, in Costar UV-transparent 96-well microplates (Corning, Inc., Corning, NY). Dityrosine formation was determined as an increase in absorbance, $\varepsilon_{315\ nm} = 8 \times 10^2\ M^{-1}\ cm^{-1}$ (*22*).

RESULTS

Inhibition of ABTS Oxidation. In our search for good model peptides to study LPO-induced dityrosine formation in proteins, we added random copolymers of glutamate and tyrosine with E/Y ratios of 4:1 (two different M_W fractions) and with an E/Y ratio of 1:1, as well as random copolymers of lysine and tyrosine ($[K_4Y_1]_{\sim 40}$), to a reaction mixture containing ABTS, LPO, and H_2O_2 (**Figure 1**). We expected that the ability of the various polymers to inhibit ABTS oxidation expressed as initial reaction rates would be an indication of the ability of the polymers to form dityrosine.

All polymers were found to be good inhibitors of LPO-mediated ABTS oxidation, as shown by the characteristic

sigmoidal inhibition curves. EC_{50} values were ~20, 50, 160, and 2.8×10^4 nM tyrosine equivalents for $[E_4Y_1]_{\sim 40}$, $[E_4Y_1]_{\sim 20}$, $[E_1Y_1]_{\sim 100}$, and $[K_4Y_1]_{\sim 40}$, respectively. Remarkably, the size of the $[E_4Y_1]_n$ polymer is seen to affect inhibition, with the higher molecular-weight polymers being more potent. The distance between tyrosine residues also affected inhibition, as was found by a comparison of the potency of $[E_4Y_1]_{\sim 40}$ and $[E_1Y_1]_{\sim 100}$. Free glutamate and tyrosine, either alone or as a mixture (molecular ratio of 4:1) did not inhibit ABTS oxidation at any concentration up to 1 mM tyrosine. The less potent inhibition observed for $[K_4Y_1]_{\sim 40}$ compared to $[E_4Y_1]_{\sim 40}$ was probably due to less favorable ionic interactions between the positively charged LPO and likewise positively charged $[K_4Y_1]_{\sim 40}$. Lower concentrations of $[K_4Y_1]_{\sim 40}$ were, however, seen to slightly promote ABTS oxidation, an effect which could be due to electron transfer from tyrsosyl radicals in $[K_4Y_1]_{\sim 40}$ to ABTS, in effect facilitating oxidation by LPO. As a control, a polymer consisting of glutamate and alanine but without tyrosine inhibited oxidation of ABTS by ~15% at 1 mM glutamate equivalents, in agreement with repulsion of the negatively charged ABTS by polymeric glutamate nonspecifically bound to LPO (data not shown).

Effect of Polymer Size on ABTS Oxidation. The difference in potency between HMW and LMW preparations of $[E_4Y_1]_n$ for inhibition of ABTS oxidation as shown in **Figure 1** was further investigated. A mixture of the HMW and LMW preparations of $[E_4Y_1]_n$ was separated by SEC into several discrete fractions (**Figure 2A**), and inhibition of ABTS oxidation was tested in the presence of the $[E_4Y_1]_n$ fractions. The resulting inhibition curves fell in two groups (**Figure 2B**): one group with the high-potency inhibitors (>10 repeating units) and one with low-potency inhibitors (<5 repeating units). Intermediate inhibition occurred with polymers consisting of 5−10 repeating units. It is also apparent from the inhibition curves that different levels of maximal inhibition were reached dependent upon polymer size. EC_{50} values for all fractions were determined (**Figure 2C**). The most potent polymers ($n > 10$) had EC_{50} values of ~20 nM, consistent with the results in **Figure 1**, and a sharp transition in potency to ~2.4 μM occurred at $5 < n < 10$.

Kinetic Study. To understand the mechanism of inhibition, the kinetics of the very potent $[E_4Y_1]_{\sim 40}$ was investigated using different concentrations of ABTS and $[E_4Y_1]_{\sim 40}$ (**Figure 3**). Analysis of the rate data in the framework of a double-reciprocal plot further showed that the polymer was a competitive inhibitor. Calculations of K_I and K_M based on the double-reciprocal plots were problematic because of the low activity in the presence of $[E_4Y_1]_{\sim 40}$. However, estimates indicated that $K_{M,\ ABTS} \sim 0.34$ mM, $V_{max\ ABTS} \sim 40$ nmol/s, and $K_{I,\ [E_4Y_1]_{\sim 40}} \sim 20$ nM.

Dityrosine Formation. Reaction of tyrosyl radicals formed by LPO in the one-electron reaction results in dimerization to yield dityrosine, and on the basis of the inhibition experiments, $[E_4Y_1]_{\sim 40}$ was expected to effectively form dityrosine. However, the results presented in **Figure 4** show that $[E_4Y_1]_{\sim 40}$ was not able to form dityrosine as analyzed by absorption spectroscopy in contrast to tyrosine. It became further clear that $[E_4Y_1]_{\sim 40}$ inhibited the formation of dityrosine from tyrosine with an EC_{50} value of 0.15 μM using 0.38 μM LPO (**Figure 4B**). This result indicates that each tyrosine unit in $[E_4Y_1]_{\sim 40}$ binds one LPO, which is more effective than indicated in **Figure 1**. Complete inhibition of LPO was not obtained, and this may be due to the reaction between polymeric tyrosine in $[E_4Y_1]_{\sim 40}$ and monomeric tyrosine, whereas the reaction between two tyrosines in the polymers is not likely due to repulsion between the negatively charged glutamate side chains. Furthermore, the inhibition seen for LPO-mediated oxidation of both ABTS and tyrosine points to specific enzyme inhibitor interactions and not direct interactions between substrates and inhibitor.

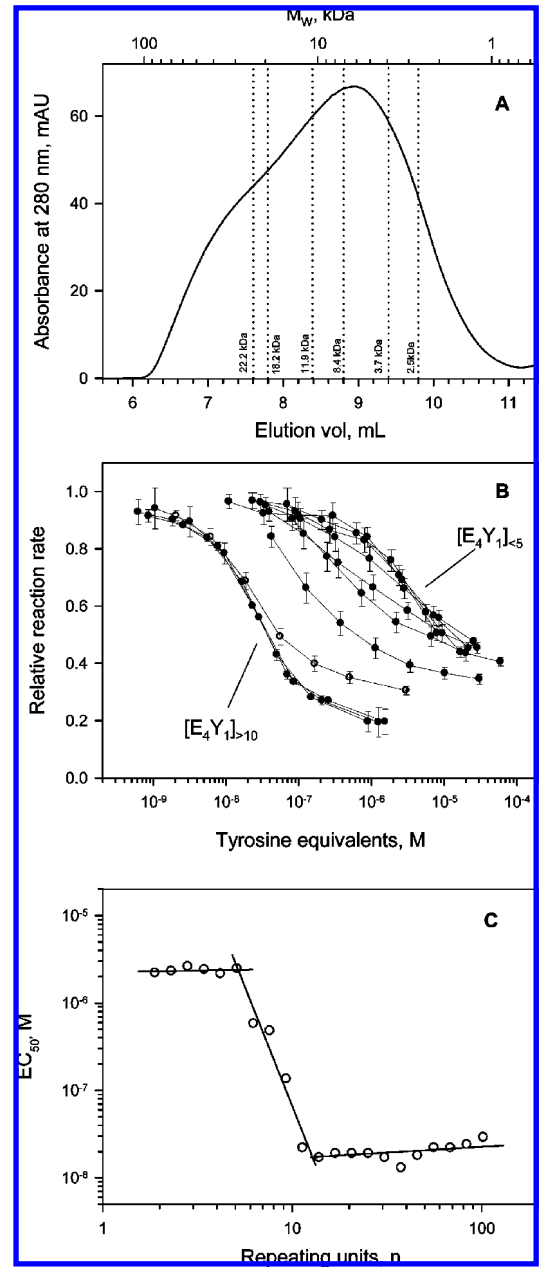

Figure 2. Effect of polymer size on the inhibition of ABTS oxidation. (A) Size-exclusion chromatography with spectrophotometric detection of high-molecular-weight and low-molecular-weight preparations of $[E_4Y_1]_n$. Molecular weights of selected fractions as determined by MALDI−TOF are indicated and used for calculation of the molecular-weight scale. The scale represents the best fit to the M_w as determined by MALDI−MS. (B) Ability of fractions to inhibit ABTS oxidation as determined by the relative rate of ABTS oxidation by hydrogen peroxide mediated by LPO in aqueous solution at pH 6.0 and 30 °C. For clarity, only selected titration curves for $[E_4Y_1]_n$ with varying n are shown. (C) EC_{50} values were calculated from the fitting of sigmoidal curves to data from B. Means ± SEM of three replicates from a representative experiment of three are shown.

Ability of $[E_4Y_1]_{\sim 40}$ To Reduce Cpd II. Cpd II could be formed by incubation of LPO with 2-fold molar excess of hydrogen peroxide. Determination of LPO activity with different peroxide concentrations (**Figure 5**) showed that *tert*-butyl hydroperoxide was nearly 3 decades poorer as a substrate

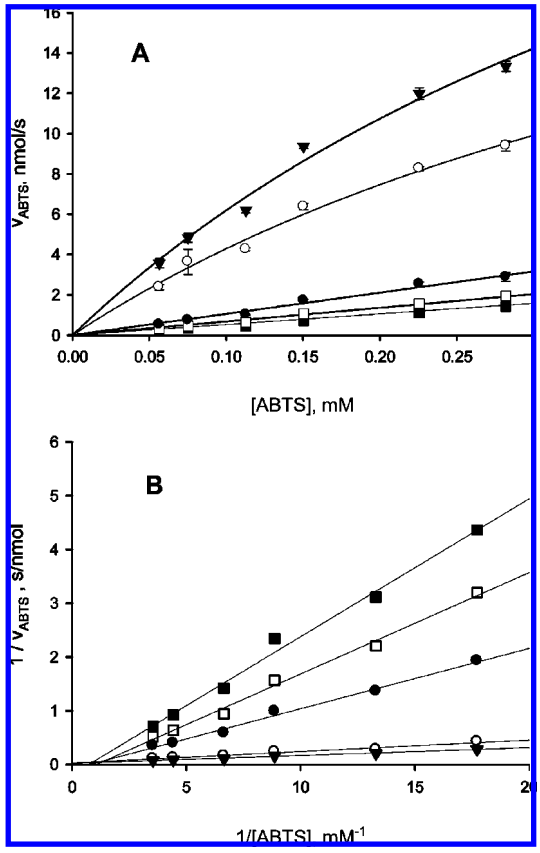

Figure 3. Rate of ABTS oxidation by hydrogen peroxide mediated by LPO in the presence of $[E_4Y_1]_{\sim 40}$ in aqueous solution with pH 6.0 at 30 °C (A) and double-reciprocal plot (B). Inhibitor concentrations were (tyrosine equivalents) 300 nM (■), 33 nM (□), 11 nM (●), 1.2 nM (○), and control (▼). Means ± SEM from three experiments are shown.

compared to hydrogen peroxide, and thus, 3.0 mM *tert*-butyl hydroperoxide was required to form Cpd II.

The reaction of tyrosine and $[E_4Y_1]_{\sim 40}$ with native LPO or preformed Cpd II was followed at the absorbance maxima of native LPO (412 nm) and Cpd II (430 nm). After initial reduction of Cpd II to native LPO following tyrosine addition, interconversion between redox intermediates at steady-state conditions occurred (**Figure 6**). The figure shows the characteristic absorption maxima of Cpd II ($t = 0$ s), native LPO after 6 s of reaction, and a spectrum taken at steady-state conditions after 200 s. As evidenced by the isosbestic point at 421 nm, only these two reaction intermediates were observed for all of the combinations of peroxide and electron donor.

In **Figure 7**, the time traces of the reaction of Cpd II or LPO with tyrosine or $[E_4Y_1]_{\sim 40}$ are shown. For clarity, only the 412 nm traces are shown. Tyrosine quickly reduced Cpd II (parts **A** and **B** of **Figure 7**) to native LPO, followed by a slow reformation of Cpd II because of the presence of excess hydrogen peroxide. The reaction of $[E_4Y_1]_{\sim 40}$ or tyrosine with Cpd II was similar when hydrogen peroxide was used as an electron acceptor (**Figure 7A**), and hence, $[E_4Y_1]_{\sim 40}$ is an apparent substrate for Cpd II. Inspection of the initial reaction between $[E_4Y_1]_{\sim 40}$ and Cpd II showed a lag phase and slower reaction only with *tert*-butyl hydroperoxide and an incomplete conversion of Cpd II to native LPO (**Figure 7B**).

The lower rate for reformation of Cpd II by $[E_4Y_1]_{\sim 40}$, as compared to tyrosine observed between 10 and 60 s (parts **A** and **C** of **Figure 7**), shows that the effect of $[E_4Y_1]_{\sim 40}$ was different from that of tyrosine.

LPO was pre-incubated with $[E_4Y_1]_{\sim 40}$ or tyrosine prior to the addition of hydrogen peroxide or *tert*-butyl hydroperoxide to investigate if $[E_4Y_1]_{\sim 40}$ was able to delay entry of peroxide to the active site (parts **C** and **D** of **Figure 7**). In the absence of an electron donor, the absorbance at 412 nm decreased to approximately 0.075 and was stable for several minutes. In the presence of tyrosine, very little Cpd II was observed because of fast conversion of Cpd II to native enzyme. In the presence of $[E_4Y_1]_{\sim 40}$, the addition of hydrogen peroxide or *tert*-butyl hydroperoxide resulted in almost complete conversion of native LPO into Cpd II as compared to the reaction in the absence of electron donor. Reduction of Cpd II occurred immediately only in the presence of hydrogen peroxide (**Figure 7C**), whereas in the presence of *tert*-butyl hydroperoxide, a much longer lag phase was observed (**Figure 7D**) and comparable to that observed when $[E_4Y_1]_{\sim 40}$ was incubated with Cpd II (**Figure 7B**).

Fluorescence measurements in parallel experiments under similar conditions as in parts **A** and **B** of **Figure 7** showed that $[E_4Y_1]_{\sim 40}$ did not form dityrosine in contrast to tyrosine. In reactions between Cpd II and $[E_4Y_1]_{\sim 40}$, fluorescence remained at the same level as before the addition of $[E_4Y_1]_{\sim 40}$. For the reaction of tyrosine and Cpd II, fluorescence increased very rapidly, almost 10-fold. Consecutive additions of the same amounts of hydrogen peroxide to the tyrosine/LPO reaction mixture resulted in a proportional fluorescence increase. A similar effect was observed for the tyrosine/LPO reaction mixture by the addition of increasing amounts of *tert*-butyl hydroperoxide, although the corresponding initial increase in fluorescence was 40-fold because of the higher peroxide concentration.

DISCUSSION

$[E_4Y_1]_n$ has previously been found not to be a substrate for LPO based on fluorescence measurements (*17*). The results presented in the present study, however, clearly show that $[E_4Y_1]_n$ is able to reduce Cpd II, although at a lower rate than tyrosine and is therefore an electron donor for LPO. Our results show that the ability of tyrosine-containing copolymers to act as inhibitors for LPO is related to polymer charge, relative content of tyrosine, and number of repeating units but that the most potent inhibitor ($[E_4Y_1]_{\sim 40}$) was not able to form dityrosine. The formation of long-lived tyrosyl-centered radicals on proteins formed by peroxidases, including LPO, has been described (*23*−*25*), but there was no direct relation to the formation of dityrosine (*24*). The ability of a specific substrate for LPO, whether it is a synthetic copolymer or a protein in milk, to form dityrosine must be related to electrostatic repulsions and size as shown here, as well as to the content of tyrosine and tertiary structure (*24*). Similar effects have been observed earlier with cationic enzymes, such as lysozyme and ribonuclease (*26, 27*), and were attributed to both electrostatic and hydrophobic interactions. In the case of LPO, it has been shown in the present study that the negative charge is not a prerequisite for inhibition, because the positively charged $[K_4Y_1]_{\sim 40}$ is also an effective inhibitor, although less potent.

Inspection of the surface charges on the barrel-shaped LPO structure published by Singh et al. (*28*) shows that it offers several positively charged binding sites for $[E_4Y_1]_n$, especially at the ends of the barrel. These positive regions could be binding sites for $[E_4Y_1]_n$ but are located 30−40 Å from the opening to the active site. Thus, when LPO is pre-incubated with $[E_4Y_1]_{\sim 40}$, Cpd II formation is not impaired with either hydrogen peroxide or *tert*-butyl hydroperoxide. In fact, the reaction of the polymer

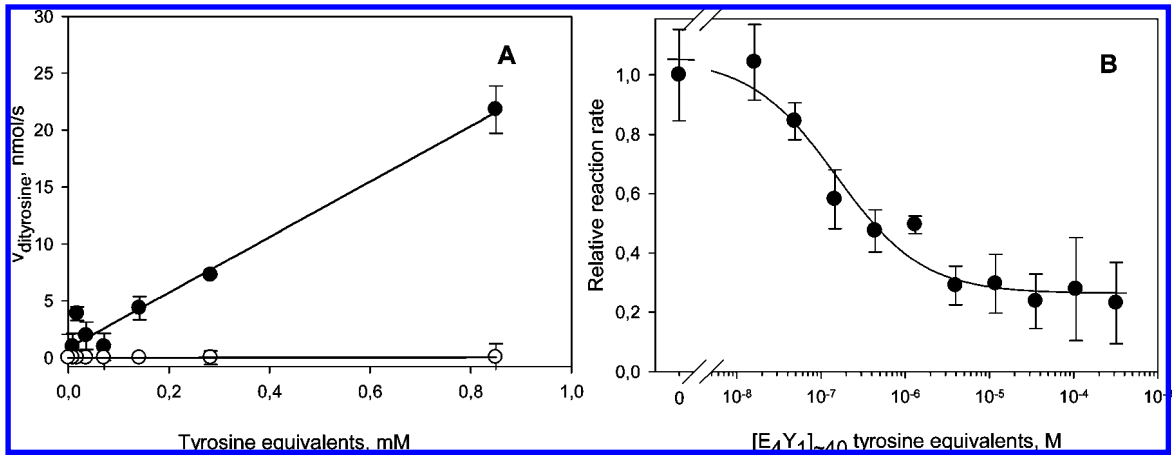

Figure 4. (A) Dityrosine formation by hydrogen peroxide mediated by LPO of tyrosine (●) and $[E_4Y_1]_{\sim 40}$ (○) at different tyrosine equivalent concentrations in aqueous solution at pH 6.0 at 30 °C, evaluated as the initial rate of dityrosine formation and (B) the inhibited dimerization from 0.5 mM tyrosine in the presence of different concentrations of $[E_4Y_1]_{\sim 40}$ expressed as the relative reaction rate. Means ± SEM from three experiments are shown.

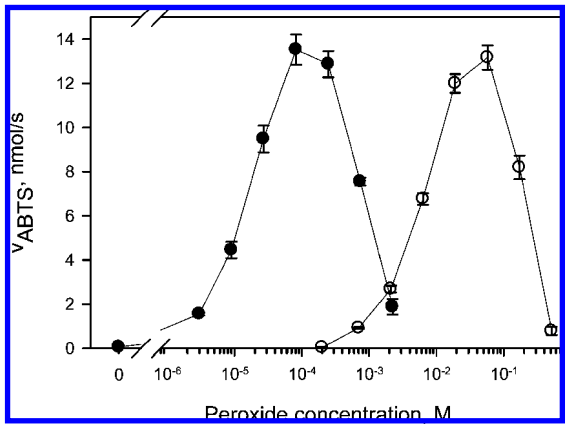

Figure 5. LPO-mediated ABTS oxidation by hydrogen peroxide (●) or *tert*-butyl hydroperoxide (○) in aqueous solution at pH 6.0 and 30 °C. Means ± SEM from three experiments are shown.

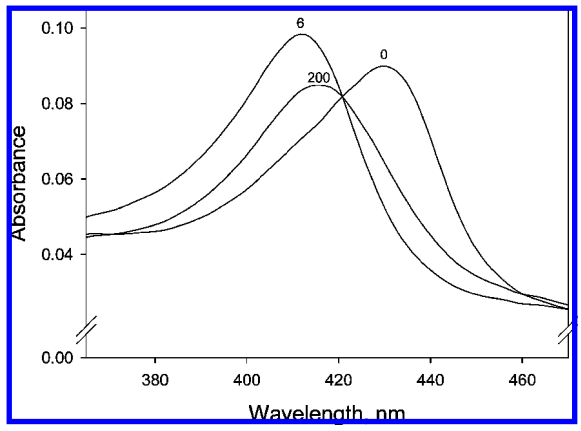

Figure 6. Absorption spectra measured during the interconversion between redox intermediates of LPO. Cpd II was formed by mixing 2.0 μM hydrogen peroxide and 1.0 μM LPO in aqueous solution at pH 6.0 and room temperature. The reaction was started by the addition of 0.2 mM tyrosine. Numbers above the spectra indicate the time of their recording and show, at $t = 0$ s, the spectrum of Cpd II ($\lambda_{max} = 430$). At $t = 6$ s, complete formation of native LPO has occurred ($\lambda_{max} = 412$). At steady-state conditions ($t = 200$ s), the primary redox intermediates are native LPO and Cpd II as evidenced by the isosbestic point at 421 nm.

with the enzyme is so slow that Cpd II is formed to the same extent as in the absence of e^- donor. Therefore, we propose that the ability of peroxides to enter the active site is not affected or blocked by $[E_4Y_1]_{\sim 40}$. On the other hand, $[E_4Y_1]_{\sim 40}$ reacts with preformed Cpd II at a rate comparable to that of tyrosine when hydrogen peroxide is used as an electron acceptor, while *tert*-butyl hydroperoxide retards the reaction between $[E_4Y_1]_{\sim 40}$ and Cpd II. This could be due to $[E_4Y_1]_{\sim 40}$ preventing *tert*-butanol from leaving the active site of LPO. Thus, we can conclude that $[E_4Y_1]_{\sim 40}$ binds tightly to LPO but does not prevent Cpd II formation. Rather, Cpd II formation might induce LPO conformational changes, exposing a hydrophobic pocket, which binds tyrosine. When hydrogen peroxide is reduced by LPO, only water needs to leave the active site, while *tert*-butanol is formed in the case of *tert*-butyl hydroperoxide.

$[E_4Y_1]_{\sim 40}$ may restrain Cpd II conformational changes that slows the escape of *tert*-butanol, resulting in a peculiar long lag phase. We expect that $[E_4Y_1]_n$ bound to Cpd II needs to displace a tyrosine unit toward the entrance to the active site. The time needed for this repositioning might explain why $[E_4Y_1]_n$ does not react as fast as tyrosine and thus allows for detectable Cpd II formation in the pre-incubation experiment. This might also be connected to the effect of polymer size, where five or fewer repeating units have a markedly lower inhibitory effect than that observed for higher molecular-weight polymers. If $[E_4Y_1]_n$ adopts an α-helical conformation (*29*), the distance between two tyrosine residues in $[E_4Y_1]_n$ will be approximately 8 Å and the length of $[E_4Y_1]_5$ will be around 40 Å. In fact, the distance from K427, which guides the opening of the substrate channel along with P234 and F239, to the nearest positively charged region on the surface of LPO approaches 30−40 Å. Thus, increasing the number of repeating units above 5 would offer a greater number of binding sites. In addition, the size of LPO might prevent binding of other enzyme molecules to the same polymer. The presence of negatively charged residues on the surface of LPO also offers binding sites for $[K_4Y_1]_{\sim 40}$; however, as we show in **Figure 1**, the lower potency may be related to the lower abundance of negatively charged regions on the surface of LPO.

McCormick et al. (*10*) showed that, in the presence of $[E_4Y_1]_n$ and tyrosine, myeloperoxidase (MPO) and horseradish peroxidase (HRP) catalyze the formation of tyrosyl radicals. The presence of free tyrosine was required by MPO for the formation of tyrosyl radicals on peptide polymers, whereas HRP formed these radicals also in the absence of tyrosine. This shows that $[E_4Y_1]_n$ is a substrate for HRP but not for MPO, despite the fact that LPO share more structural and catalytic properties with MPO than HRP (*30*−*32*). Both LPO and MPO probably act

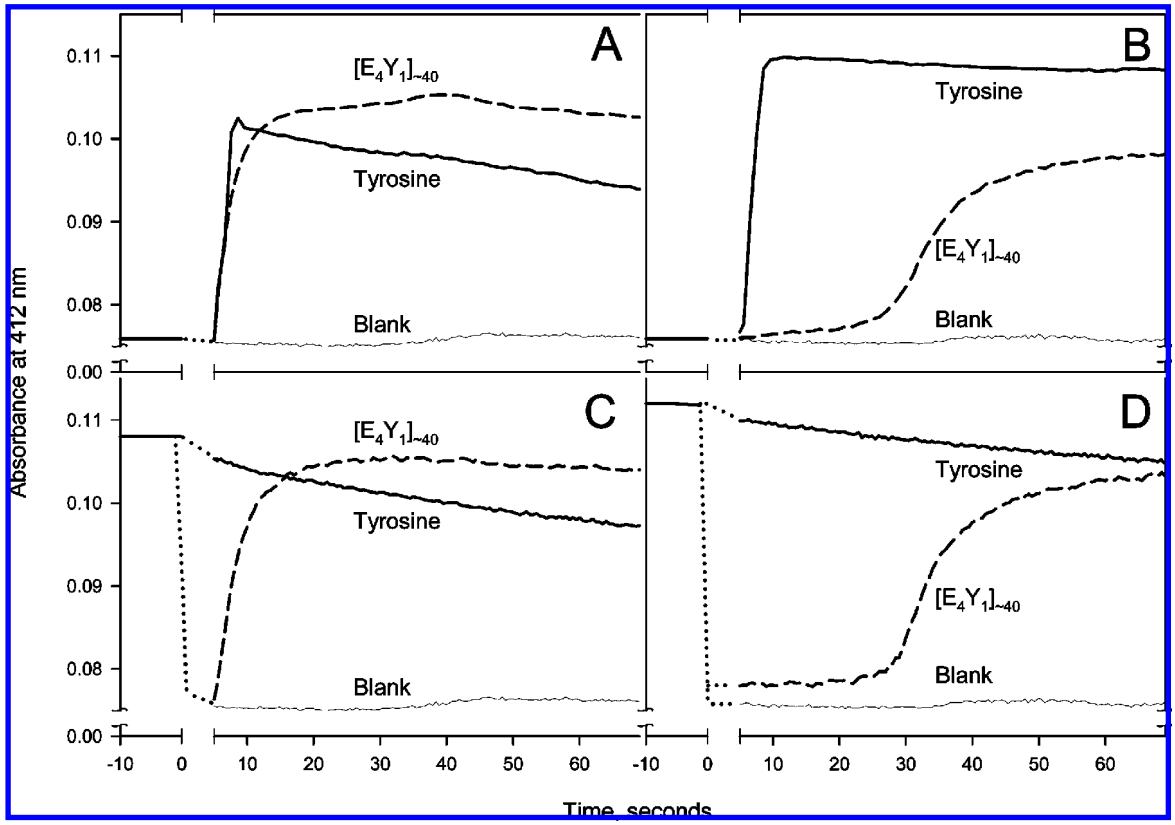

Figure 7. Reaction of Cpd II with tyrosine (—) or $[E_4Y_1]_{\sim 40}$ (- - -) (A and B) and reaction of native LPO with H_2O_2 or *tert*-butyl hydroperoxide after incubation with tyrosine or $[E_4Y_1]_{\sim 40}$ (C and D) in aqueous solution at pH 6.0 and room temperature as determined by measurement of native LPO at 412 nm. Hydrogen peroxide (A and C) or *tert*-butyl hydroperoxide (B and D) were used as electron acceptors. For comparison, time traces of Cpd II formed with H_2O_2 or *tert*-butyl hydroperoxide in the absence of electron donor (blank) are shown (——). Peroxide (A and B) or electron donor (C and D) was added at $t = 0$. The dotted lines indicate that the initial events were not determined experimentally. Experiments were repeated 3 times with similar results.

catalytically through a proton relay mechanism; however, the opening of the substrate channel of LPO is guided by K427, P234, and F239, whereas in MPO, the corresponding residues are G412, D218, and L223. Furthermore, two other positively charged residues are located within 20 Å on the surface of LPO, while in MPO, two negatively charged residues are located close to the opening (*28*).

Oxidation of polymeric tyrosine in $[E_4Y_1]_n$ without subsequent formation of dityrosine implies the existence of free tyrosyl radicals that then may oxidize cysteine residues (*33*) or other tyrosine residues. LPO contains only one free cysteine, which is located in the interior of the enzyme (*28, 34*) and is therefore not likely to be oxidized. Di- and trimerization of LPO is known to occur through the formation of intermolecular dityrosine cross-linking, which could be induced by the presence of free tyrosyl radicals (*24, 35*). However, using direct spectrophotometric and fluorometric detection, we were not able to detect dityrosine formed by LPO in the presence of $[E_4Y_1]_{\sim 40}$. If lipids are present, these radicals may induce other oxidative processes, such as peroxidation (*36, 37*).

We propose that the mechanism for inhibition of LPO by $[E_4Y_1]_n$ is due to ionic interactions between the negatively charged glutamate residues of the substrate and positively charged regions on LPO. Polymer size is crucial for inhibition, and this may be related to the position of major binding sites for $[E_4Y_1]_n$ relatively far from the opening to the substrate channel.

ABBREVIATIONS USED

ABTS, 2,2′-azino-bis(3-ethylbenzthiazoline-6-sulfonic acid); Cpd, compound; LMW, low molecular weight; LPO, lactoperoxidase; HMW, high molecular weight; HRP, horseradish peroxidase; MALDI−TOF, matrix-assisted laser desorption−ionization time-of-flight; MPO, myeloperoxidase; SEC, size-exclusion chromatography.

LITERATURE CITED

(1) Thomas, E. L.; Bozeman, P. M.; Learn, D. B. Lactoperoxidase: Structure and catalytic properties. In *Peroxidases in Chemistry and Biology*; Everse, J., Everse, K. E., Grisham, M. B., Eds.; CRC Press: Boca Raton, FL, 1991.

(2) Monzani, E.; Gatti, A. L.; Profumo, A.; Casella, L.; Gullotti, M. Oxidation of phenolic compounds by lactoperoxidase. Evidence for the presence of a low-potential compound II during catalytic turnover. *Biochemistry* **1997**, *36*, 1918–1926.

(3) Aeschbach, R.; Amado, R.; Neukom, H. Formation of dityrosine cross-links in proteins by oxidation of tyrosine residues. *Biochim. Biophys. Acta* **1976**, *439*, 292–301.

(4) Kumar, K. S.; Walls, R.; Hochstein, P. Lipid peroxidation and hemolysis induced by lactoperoxidase and thyroid hormones. *Arch. Biochem. Biophys.* **1977**, *180*, 514–521.

(5) Lovaas, E. Free radical generation and coupled thiol oxidation by lactoperoxidase/SCN^-/H_2O_2. *Free Radical Biol. Med.* **1992**, *13*, 187–195.

(6) Buege, J. A.; Aust, S. D. Lactoperoxidase-catalyzed lipid peroxidation of microsomal and artificial membranes. *Biochim. Biophys. Acta* **1976**, *444*, 192–201.

(7) Sun, S. N.; Bao, Z. J.; Ma, H. M.; Zhang, D. Q.; Zheng, X. P. Singlet oxygen generation from the decomposition of α-linolenic acid hydroperoxide by cytochrome *c* and lactoperoxidase. *Biochemistry* **2007**, *46*, 6668–6673.
(8) Ghibaudi, E.; Laurenti, E. Unraveling the catalytic mechanism of lactoperoxidase and myeloperoxidase. *Eur. J. Biochem.* **2003**, *270*, 4403–4412.
(9) Furtmuller, P. G.; Zederbauer, M.; Jantschko, W.; Helm, J.; Bogner, M.; Jakopitsch, C.; Obinger, C. Active site structure and catalytic mechanisms of human peroxidases. *Arch. Biochem. Biophys.* **2006**, *445*, 199–213.
(10) McCormick, M. L.; Gaut, J. P.; Lin, T. S.; Britigan, B. E.; Buettner, G. R.; Heinecke, J. W. Electron paramagnetic resonance detection of free tyrosyl radical generated by myeloperoxidase, lactoperoxidase, and horseradish peroxidase. *J. Biol. Chem.* **1998**, *273*, 32030–32037.
(11) Childs, R. E.; Bardsley, W. G. The steady-state kinetics of peroxidase with 2,2′-azino-di-(3-ethyl-benzthiazoline-6-sulphonic acid) as chromogen. *Biochem. J.* **1975**, *145*, 93–103.
(12) Shindler, J. S.; Childs, R. E.; Bardsley, W. G. Peroxidase from human cervical mucus. The isolation and characterisation. *Eur. J. Biochem.* **1976**, *65*, 325–331.
(13) Shindler, J. S.; Bardsley, W. G. Steady-state kinetics of lactoperoxidase with ABTS as chromogen. *Biochem. Biophys. Res. Commun.* **1975**, *67*, 1307–1312.
(14) Bardsley, W. G. Steady-state kinetics of lactoperoxidase-catalyzed reactions. In *The Lactoperoxidase System, Chemistry and Biological Significance*; Pruitt, K. M., Tenovuo, J., Eds.; Marcel Dekker, Inc.: New York, 1985.
(15) Braun, S.; Abdel, G. M.; Lettieri, J. A.; Racker, E. Partial purification and characterization of protein tyrosine kinases from normal tissues. *Arch. Biochem. Biophys.* **1986**, *247*, 424–432.
(16) Braun, S.; Raymond, W. E.; Racker, E. Synthetic tyrosine polymers as substrates and inhibitors of tyrosine-specific protein kinases. *J. Biol. Chem.* **1984**, *259*, 2051–2054.
(17) Malencik, D. A.; Anderson, S. R. Dityrosine formation in calmodulin: Cross-linking and polymerization catalyzed by *Arthromyces* peroxidase. *Biochemistry* **1996**, *35*, 4375–4386.
(18) Wetlaufer, D. B.; Edsall, J. T.; Hollingworth, B. R. Ultraviolet difference spectra of tyrosine groups in proteins and amino acids. *J. Biol. Chem.* **1958**, *233*, 1421–1428.
(19) Paul, K. G.; Ohlsson, P. I. The lactoperoxidase system. In *The Lactoperoxidase System, Chemistry and Biological Significance*; Pruitt, J. O., Tenovuo, J. O., Eds.; Marcel Dekker: New York, 1985.
(20) Nelson, D. P.; Kiesow, L. A. Enthalpy of decomposition of hydrogen peroxide by catalase at 25 °C (with molar extinction coefficients of H_2O_2 solutions in the UV). *Anal. Biochem.* **1972**, *49*, 474–478.
(21) Kohler, H.; Taurog, A.; Dunford, H. B. Spectral studies with lactoperoxidase and thyroid peroxidase—Interconversions between native enzyme, compound II, and compound III. *Arch. Biochem. Biophys.* **1988**, *264*, 438–449.
(22) Bayse, G. S.; Michaels, A. W.; Morrison, M. The peroxidase-catalyzed oxidation of tyrosine. *Biochim. Biophys. Acta* **1972**, *284*, 34–42.
(23) Østdal, H.; Skibsted, L. H.; Andersen, H. J. Formation of long-lived protein radicals in the reaction between H_2O_2-activated metmyoglobin and other proteins. *Free Radical Biol. Med.* **1997**, *23*, 754–761.
(24) Østdal, H.; Bjerrum, M. J.; Pedersen, J. A.; Andersen, H. J. Lactoperoxidase-induced protein oxidation in milk. *J. Agric. Food Chem.* **2000**, *48*, 3939–3944.
(25) Østdal, H.; Andersen, H. J.; Davies, M. J. Formation of long-lived radicals on proteins by radical transfer from heme enzymes—A common process. *Arch. Biochem. Biophys.* **1999**, *362*, 105–112.
(26) Sela, M. Inhibition of ribonuclease by copolymers of glutamic acid and aromatic amino acids. *J. Biol. Chem.* **1962**, *237*, 418–421.
(27) Sela, M.; Steiner, L. A. Inhibition of lysozyme by some copolymers of amino acids. *Biochemistry* **1963**, *2*, 416–421.
(28) Singh, A. K.; Singh, N.; Sharma, S.; Singh, S. B.; Kaur, P.; Bhushan, A.; Srinivasan, A.; Singh, T. Crystal structure of lactoperoxidase at 2.4 Å resolution. *J. Mol. Biol.* **2008**, *376*, 1060–1075.
(29) Trudelle, Y.; Spach, G. Circular dichroism study of poly(L-tyrosine), poly(L-glutamic acid) and of random and sequential copolymers of L-glutamic acid and L-tyrosine in trimethylphosphate. *Polymer* **1975**, *16*, 16–20.
(30) Zederbauer, M.; Furtmueller, P. G.; Brogioni, S.; Jakopitsch, C.; Smulevich, G.; Obinger, C. Heme to protein linkages in mammalian peroxidases: Impact on spectroscopic, redox and catalytic properties. *Nat. Prod. Rep.* **2007**, *24*, 571–584.
(31) Poulos, T. L.; Fenna, R. E. Peroxidases: Structure, function, and engineering. In *Metalloenzymes Involving Amino Acid-Residue and Related Radicals*; Sigel, H., Sigel, A., Eds.; Marcel Dekker, Inc.: New York, 1994.
(32) Jantschko, W.; Furtmuller, P. G.; Allegra, M.; Livrea, M. A.; Jakopitsch, C.; Regelsberger, G.; Obinger, C. Redox intermediates of plant and mammalian peroxidases: A comparative transient-kinetic study of their reactivity toward indole derivatives. *Arch. Biochem. Biophys.* **2002**, *398*, 12–22.
(33) Bhattacharjee, S.; Deterding, L. J.; Jiang, J.; Bonini, M. G.; Tomer, K. B.; Ramirez, D. C.; Mason, R. P. Electron transfer between a tyrosyl radical and a cysteine residue in hemoproteins: Spin trapping analysis. *J. Am. Chem. Soc.* **2007**, *129*, 13493–13501.
(34) DeGioia, L.; Ghibaudi, E. M.; Laurenti, E.; Salmona, M.; Ferrari, R. P. A theoretical three-dimensional model for lactoperoxidase and eosinophil peroxidase, built on the scaffold of the myeloperoxidase X-ray structure. *J. Biol. Inorg. Chem.* **1996**, *1*, 476–485.
(35) Lardinois, O. M.; Medzihradszky, K. F.; de Montellano, P. R. O. Spin trapping and protein cross-linking of the lactoperoxidase protein radical. *J. Biol. Chem.* **1999**, *274*, 35441–35448.
(36) Heinecke, J. W. Tyrosyl radical production by myeloperoxidase: A phagocyte pathway for lipid peroxidation and dityrosine cross-linking of proteins. *Toxicology* **2002**, *177*, 11–22.
(37) Savenkova, M. L.; Mueller, D. M.; Heinecke, J. W. Tyrosyl radical generated by myeloperoxidase is a physiological catalyst for the initiation of lipid peroxidation in low density lipoprotein. *J. Biol. Chem.* **1994**, *269*, 20394–20400.

Received for review May 21, 2008. Revised manuscript received July 23, 2008. Accepted August 6, 2008. This study was supported by Alltech Biotechnology, Inc., Lexington, KY, and LMC Research School FOOD, Denmark.

JF801582E